

On the Inherent Robustness of One-Stage Object Detection against Out-of-Distribution Data

Aitor Martinez-Seras^{a,b,*}, Javier Del Ser^{a,c}, Alain Andres^{a,b},
Pablo Garcia-Bringas^b

^a*TECNALIA, Basque Research and Technology Alliance (BRTA), 48160 Derio, Spain*

^b*University of Deusto, 48007 Bilbao, Spain*

^c*University of the Basque Country (UPV/EHU), 48013 Bilbao, Spain*

Abstract

Robustness is a fundamental aspect for developing safe and trustworthy models, particularly when they are deployed in the open world. In this work we analyze the inherent capability of one-stage object detectors to robustly operate in the presence of out-of-distribution (OoD) data. Specifically, we propose a novel detection algorithm for detecting unknown objects in image data, which leverages the features extracted by the model from each sample. Differently from other recent approaches in the literature, our proposal does not require retraining the object detector, thereby allowing for the use of pretrained models. Our proposed OoD detector exploits the application of supervised dimensionality reduction techniques to mitigate the effects of the curse of dimensionality on the features extracted by the model. Furthermore, it utilizes high-resolution feature maps to identify potential unknown objects in an unsupervised fashion. Our experiments analyze the Pareto trade-off between the performance detecting known and unknown objects resulting from different algorithmic configurations and inference confidence thresholds. We also compare the performance of our proposed algorithm to that of logits-based post-hoc OoD methods, as well as possible fusion strategies. Finally, we discuss on the competitiveness of all tested methods against state-of-the-art OoD approaches for object detection models over the recently published Unknown Object Detection benchmark. The obtained results verify that the

*Corresponding author. Parque Tecnológico de Bizkaia, 700, 48160 Derio, Bizkaia, Spain. Phone: +34946430850.

Email address: aitor.martinez@tecnalia.com (Aitor Martinez-Seras)

performance of avant-garde post-hoc OoD detectors can be further improved when combined with our proposed algorithm.

Keywords:

Safe Artificial Intelligence, Trustworthy Artificial Intelligence, Open-World Object Detection, Out-of-Distribution Detection

1. Introduction

The rapid advancement and widespread adoption of Artificial Intelligence (AI) systems for real-world applications have underscored the urgent need for these models to be safe and trustworthy [1]. What trustworthiness means for AI is a highly debated concern in the recent years, attracting significant interest from the research community. A major breakthrough in shedding light on trustworthy AI was the publication of the “Ethical Guidelines for Trustworthy AI” [2] in 2019 by the European Union, a regulatory actor of relevance in this matter. The text outlines seven key requirements for trustworthy AI and identify three essential pillars for fulfilling these requirements. The *technical robustness and safety* of an AI system is recognized as one of the seven requirements and a fundamental pillar of trustworthiness [3]. More recently, another important actor in the regulatory landscape, the National Institute of Standards and Technology (NIST) has defined in [4] the technical robustness as a system’s capacity to sustain its performance across diverse conditions. It entails not only consistent functioning under anticipated scenarios, but also the ability to minimize potential risks to individuals when operating in environments subject to unexpected events.

For this purpose, ensuring the safety of Machine Learning (ML) models involves developing robust systems capable of handling unknown semantics, effectively distinguishing between known and unknown data instances. When it comes to object detection tasks from image data, these models must be able to navigate open-world environments by discerning between background (irrelevant information), known objects (relevant information within the training distribution), and unknown objects (relevant information outside the training distribution). In this context, substantial efforts have been directed towards the field of Open World Object Detection (OWOD) [5]-[8]. The goal pursued in this research area is to develop models capable of detecting unknown objects and incrementally learning new categories over time. Predominantly, research in this area has concentrated on methodolo-

gies that require retraining two-stage object detection models, such as Faster R-CNN. Different retraining strategies are designed to endow the learned model with the capability to discern a broader variety of objects (including those not present in the training data), such as continual learning approaches or loss functions related to the presence of objects (*objectness*). Conversely, pretrained object detection models require less computational power when compared to retrained models because they are optimized on a fixed dataset of known classes. However, this efficiency comes at the cost of increased bias towards detecting only familiar objects, making them less suitable for open-world scenarios where new, unseen objects may appear.

This manuscript contributes to understanding the robustness of pretrained object detection models in detecting unknown objects in image data. We depart from our hypothesis that, without retraining, single-stage object detection models can inherently detect unknown objects. To explore this, we introduce a simple OoD detection algorithm based on neural activations (*feature maps*) of pretrained models. Additionally, we present an unsupervised learning method that leverages feature maps to enhance recall for unknown objects. Our extensive experimental setup evaluates the algorithm across different configurations and parameter choices, assessing its effectiveness in identifying known and unknown objects compared to logits-based OoD methods and retrained object detection models. We further explore potential improvements through a fusion of tested methods, inspired by findings in [9]. Finally, we compare our approach with state-of-the-art OWOD methods, showing that the proposed algorithm achieves superior detection scores in the benchmark without requiring model retraining.

The remainder of the paper is organized as follows: Section 2 revisits OoD detection techniques for object detection, along with a brief summary of the most influential works in OWOD and a detailed statement of the contribution brought by this work to the related literature. Section 3 presents and describes our algorithm for detecting unknown objects¹ in images, beginning with an overview of its compounding algorithmic steps, and followed by a detailed description of the method. This section also introduces two techniques aimed at enhancing the overall performance of the algorithm. The experimental setup is outlined in Section 4, whereas the results are analyzed and discussed in Section 5. Finally, Section 6 concludes the manuscript with

¹Throughout this work “unknown object” and “OoD object” are used interchangeably.

a summary of the main findings and an outlook towards potential research paths to be addressed in the future.

2. Related Work and Contribution

This section provides an overview of existing OoD techniques tailored for object detection (Subsection 2.1), reviews key works within the OWOD framework (Subsection 2.2), and presents this paper’s contributions to the OoD literature (Subsection 2.3).

2.1. Out-of-Distribution Detection in Object Detection

As noted in the introduction, the goal of OoD detection is to identify unknown samples in classification tasks—specifically, samples with semantics not present in the training distribution. Numerous techniques have been proposed in this area. e.g., ReAct [10], GradNorm [11], MSP [12], ODIN [13] or Energy [14]. These techniques were originally conceived for detecting OoD data in image classification tasks. In object detection tasks, however, OoD detection refers to the model’s ability to locate and identify objects in an image that do not belong to any of the classes it was trained to recognize. While traditional object detection models are trained to detect a fixed set of classes, OoD detection enables these models to recognize when an object falls outside this known set, flagging it as *unknown*.

Due to its higher complexity than in traditional image classifier, the detection of unknowns in object detection models has garnered increasing interest during the last couple of years. Several methods devised to cope with this problem have been reported in the literature, such as those presented in [15] and [16]. Both are focused on regularizing a two-stage object detection model via the usage of unknowns. In the former, Virtual Outlier Synthesis (VOS) technique is proposed to synthesize virtual outliers in the feature space, without relying on external data to allow the model to better learn the boundaries between known and unknown classes. In the latter, the same objective is pursued. Differently, unknowns are obtained or distilled from videos leveraging contiguous frames and a dissimilarity metric based on the L_2 distance between features of the object proposals.

Another example is [17], where authors propose a post-hoc OoD detector for object detection that utilizes Sensitivity-Aware FEatures (SAFE) extracted from residual convolutional layers and abnormal batch normalization activations. SAFE extracts object-specific feature vectors and employs a

multilayer perceptron trained on the surrogate task of distinguishing adversarially perturbed samples from clean samples to classify each detected object as in-distribution or OoD. Finally, the work in [18] does not directly perform OoD detection in an object detection task. Instead, they leverage concepts from object detection to perform OoD detection in multi-label classification tasks. They convert a regular object detection model (YOLO) into an image classifier with inherent OoD detection capabilities by exploiting the model’s ability to distinguish between objects of interest and irrelevant objects.

2.2. Open-World Object Detection Framework

The OWOD framework was introduced by [5] to address the limitations of traditional object detection models that assume all object classes are known during training. In the open-world setting, a model is expected to not only detect known objects but also identify unknown objects that do not belong to the training classes. The evaluation protocol established was based on the concepts and metrics introduced in [19]. It consist of grouping the classes of into sequential tasks, where each task introduces new classes incrementally and the not-yet-included classes are treated as the unknowns to be detected. This protocol is based on the `PASCAL VOC` [20] and `COCO` [21] datasets, which are two of the most commonly used benchmark datasets in object detection. All `PASCAL` classes and data are considered to be the first task. The remaining 60 classes of `COCO` are grouped into three successive tasks with semantic drifts that are incrementally introduced to simulate the unknowns arriving at the model’s input. Since its inception, this evaluation protocol has been adopted by most contributions dealing with open-world object detection tasks.

In the literature related to OWOD, it is important to note that most methods proposed to date hinge on the addition of an “unknown” class to a two-stage object detection model. This newly added class is trained using pseudo-labels obtained by several heuristics or techniques. Thereupon, each contribution to the literature following this approach introduces different algorithmic updates to the training algorithm to improve the performance of the model over the “unknown” class, while preserving the detection capabilities on the known classes.

The solution proposed in [5] called ORE uses contrastive clustering, an unknown-aware proposal network and an energy-based unknown identification to address the challenges of open-world detection. This way ORE is able to predict unknown objects as “unknown” and incrementally learn new classes as their labels become available, without forgetting previously learned

classes. Building on this work, [6] proposed a method called ORDER for addressing the challenges of detecting both known and unknown objects in road scenes. The authors introduce Feature-Mix, which improves unknown object detection by mixing features of known and unknown objects at the feature level. Additionally, they propose a focal regression loss to address intra-class scale variation and improve small object detection. The model is further improved through curriculum learning and is evaluated on the BDD and IDD road scene datasets.

Contrary to previous approaches, the work done in [22] introduces a novel end-to-end transformer-based framework for open-world object detection called OW-DETR. It comprises three dedicated components to address the challenges of OWOD, specifically attention-driven pseudo-labeling, novelty classification, and objectness scoring. The attention-driven pseudo-labeling scheme selects object query boxes with high attention scores as potential unknown objects, which are then used along with ground-truth known objects to train a novelty classifier. The objectness branch aims to effectively separate foreground objects (known and pseudo-unknown) from the background by enabling knowledge transfer from known to unknown classes. Finally, the novelty classification branch is in charge of distinguishing the pseudo unknowns from each of the known classes.

Authors in [7] point out that while the prior OWOD work introduced the problem definition, the experimental settings were unreasonable, the metrics were incomplete and the methodology was inappropriate. To address these issues, the paper proposes five fundamental benchmark principles to guide the construction of OWOD benchmarks. Furthermore, the authors present a novel OWOD method that includes an auxiliary proposal advisor module based on a selective search algorithm [23] to assist the RPN in identifying accurate unknown proposals by the addition of unsupervised information, and a class-specific expelling classifier to calibrate overconfident predictions and to filter out confusing outputs.

The work in [24] goes one step beyond previous OWOD approaches by not only aiming to detect unknown instances, but also by classifying them into different unknown classes. First, an unknown label-aware proposal module and an unknown-discriminative classifier head are used to detect known and unknown objects. Then, similarity-based unknown classification and unknown clustering refinement modules are constructed to distinguish among multiple unknown classes.

A common problem to above introduced approaches is that the module

generating the proposals for the unknown objects (namely, the RPN in two-stage object detectors) is highly biased towards detecting known objects as it is the only ground truth available in the training data. To mitigate this bias, [8] substitutes the RPN with random region proposals that prevents the training from being confounded by the limited known object classes. Additionally, the authors introduce a matching score that does not penalize random proposals whose predictions do not match the known classes, encouraging the exploration of unknown objects all over the image.

Finally, the authors in [25] address exclusively the initial stage of the OWOD framework, focusing solely on the identification of unknown objects. They evaluate their method using their proposed Unknown Object Detection (UOD) benchmark, which is derived from two small subsets of the COCO dataset, augmented with annotations for unknown objects. These new annotations are generated by them and their team. The evaluation protocol involves assessing the models only on one task within these two subsets, without any incremental addition of new classes to the model. The authors also propose the so-called unknown sniffer model, which introduces a Generalized Object Confidence (GOC) score to avoid improper suppression of unknowns. Similarly, a negative energy suppression loss is used to further suppress non-object samples in the background. To obtain the best bounding box for unknown objects during inference, the paper presents a graph-based determination scheme to replace the non-maximum suppression (NMS) post-processing.

2.3. Contribution

In the light of the reviewed OWOD literature, it becomes evident that there is a clear trend towards using two-stage models that undergo retraining to acquire the capability to detect unknown objects. To avoid this computational burden, it is imperative to analyze the performance of OoD techniques for one-stage models which do not require retraining of the object detection model. In our research, we align our approach with the work of [25], by focusing exclusively on the first task of OWOD (the ability to detect unknown objects), without subsequently retraining the model with these newly identified classes. Our contributions in this regard can be summarized as follows:

- *We explore the effectiveness of classic post-hoc OoD techniques on one-stage object detectors.* Specifically, we investigate the performance of tra-

ditional post-hoc OoD methods when applied to one-stage object detection models, which are generally more efficient but less studied in this context.

- *We propose a simple OoD technique based on feature maps that does not require retraining.* We introduce a straightforward and computationally efficient method for detecting unknown objects that leverages feature maps within one-stage detector object detection models. This technique is designed to operate without the need for retraining, hence having no impact on the overall training complexity and maintaining the naive capability of the model to detect and identify known objects.
- *We propose techniques for enhancing detection of potential unknown objects using feature maps.* We experiment with various methods to improve the detection of unknown objects by utilizing feature maps. This includes refining feature extraction and leveraging advanced techniques to better identify and classify OoD objects.
- *We examine the potential of fusing OoD methods to robustly identify unknown objects.* We explore the benefits of combining different OoD detection methods in the form of a detection ensemble, aiming to complement each other when deciding on the known or unknown nature of an object. Similarly to supervised learning ensembles, fusing OoD methods can yield more robust OoD detection capabilities for the overall model than every one of them in isolation.

Ultimately, our research work contributes to the understanding and development of more effective OoD detection techniques for one-stage object detectors, leading to more robust and adaptable models for object detection in open-world scenarios.

3. Open-World Object Detection by Feature Map Characterization

In this section we introduce our proposed OoD detection algorithm which, given its reliance on the feature maps within the model, is hereafter referred to as the FMap detector. Subsection 3.1 presents the general workflow of FMap, while Subsection 3.2 details in depth each of its compounding algorithmic steps. Next, Subsection 3.3 elaborates on the benefits of employing Supervised Dimensionality Reduction (SDR) with our detector. Finally, Subsection 3.4 outlines an approach to enhance the capabilities for identifying

unknown objects without penalizing the performance in detecting known objects.

3.1. High-level Description of FMap

We begin by pausing at the general workflow followed by FMap, which is illustrated in Figure 1. In essence, FMap characterizes the activation space at the output of a single-stage object detection model, i.e., we characterize the feature maps computed by the model for its input. In doing so, it is important to first note that modern single-stage object detection models employ a Feature Pyramid Network (FPN) [26] to enhance their ability to detect objects at various scales. Therefore, the characterization of activations made by FMap must account for this feature. In the case of two-stage detectors, feature maps of different strides are merged and standardized to have a uniform number of output channels or dimensions after the FPN. In contrast, mainstream one-stage detectors do not perform this standardization, resulting in each stride having unique dimensions and producing predictions independently.

Since FMap is tailored for one-stage detectors, each stride is characterized separately within its own space as each prediction emanates from only one of the strides. This means that features from different strides are processed by distinct layers, and hence may not share the same number of dimensions or the same semantic meaning. The workflow of FMap comprises the following steps:

1. First FMap iterates over the in-distribution (ID) data – namely, the training dataset – to collect all the extracted feature maps of objects correctly predicted by the trained model, together with the stride from which each object prediction is produced.
2. Subsequently, for each class and stride, we cluster its embedding space and aggregate all object embeddings inside every cluster into a centroid, which is done by computing the mean of every feature within the cluster. This yields multiple centroids for each class in each stride, serving as the representatives of the concepts in the embedding space corresponding to that class.
3. The score for each query sample is defined as the minimum distance of the instance’s features to the centroids of the predicted class in the respective stride (since each prediction originates from only one stride). Based on

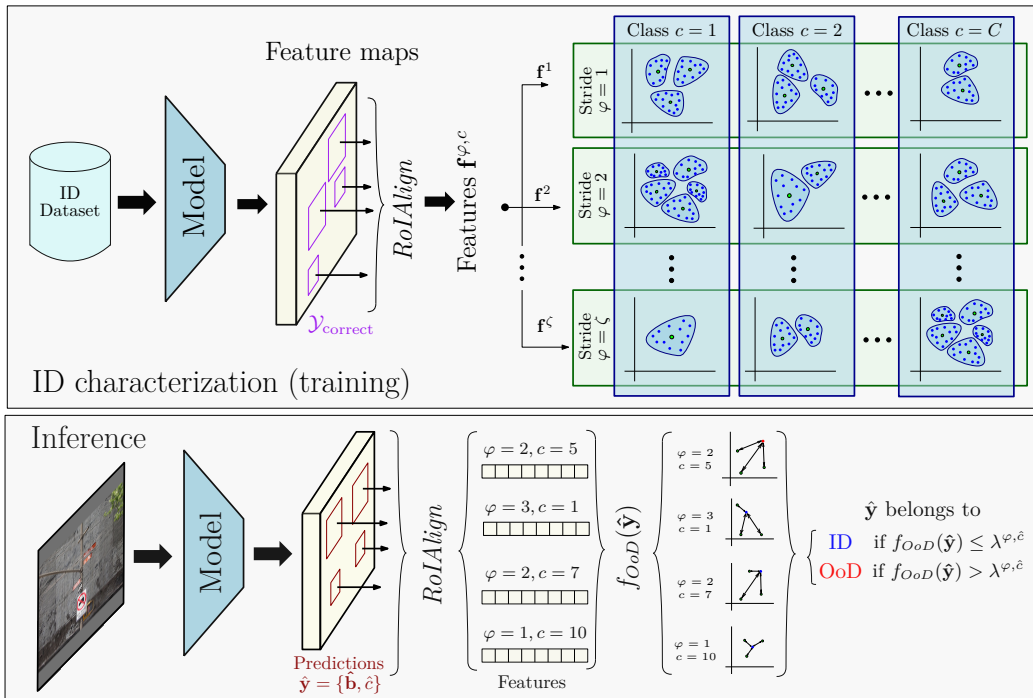


Figure 1: Block diagram describing the general operation of the proposed FMap detector. In the inference part, an example for the stride (φ) and class (c) values is displayed.

this definition, to determine whether a query sample is an OoD instance, we first establish a threshold for the aforementioned score. To this end, we iterate again over the ID data to obtain the scores for the correctly predicted instances. Each class in each stride will have its own ID score distribution and corresponding threshold $\lambda^{\varphi,c}$.

4. Finally, we establish the threshold value to that such that a desired True Positive Rate (TPR) is achieved for each class in each stride independently, ensuring that a specified number of ID samples are correctly classified as ID.

This computed threshold $\lambda^{\varphi,c}$ for every (class, stride) pair is used during inference to determine whether each prediction issued by the object detector belongs to the in-distribution or, instead, must be declared as an unknown object. The next subsection provides further mathematical details on this inference process.

3.2. Low-level Description of FMap

This section provides a more detailed description of the FMap detector, along with a schematic summary in Algorithm 1. As previously mentioned, the first step is to characterize the ID by creating the representative features or centroids of each class in each stride by making use of clustering techniques. Hence, we start extracting the features from the ID samples by iterating over the training dataset \mathcal{D}_{tr} and collecting the predictions. The dataset consists of images $\mathbf{x} \in \mathbb{R}^{W \times H \times C}$ with objects represented by targets $\mathbf{y} = \{\mathbf{b}, c\}$, where $\mathbf{b} \in \mathbb{R}^4$ denotes the bounding box coordinates and $c \in \{1, 2, \dots, C\}$ the class or category of the object. C represents the number of classes in \mathcal{D}_{tr} . Each image can contain one or multiple targets (labeled objects). Among all the predictions $\hat{\mathbf{y}} = \{\hat{\mathbf{b}}, \hat{c}\}$ generated by the model, only the correctly predicted ones are considered for feature extraction, i.e., $\mathcal{Y}_{\text{correct}} = \{\hat{\mathbf{y}} \text{ such that } \hat{c} = c \text{ and } \text{IoU}(\hat{\mathbf{b}}, \mathbf{b}) \geq \Gamma_{\text{IoU}}\}$, where IoU denotes *Intersection over Union* and $\Gamma_{\text{IoU}} \in \mathbb{R}(0, 1)$ is a predefined threshold. Features $\mathbf{f} \in \mathbb{R}^{D_\varphi}$ are extracted from the feature maps \mathbf{v} , where D_φ represents the dimensionality of the stride indexed by $\varphi \in \{1, 2, \dots, \zeta\}$ being ζ the total number of strides (line 5 of Algorithm 1).

To perform the extraction of the features corresponding to each prediction, we utilize the *RoIAlign* operation as described in [27]. The inputs are a bounding box \mathbf{b} , the desired output size (height and width) for the features \mathbf{f} of the box, the complete feature maps \mathbf{v} , and the ratio between the spatial resolution of the bounding boxes (height and width of the original image) and the spatial resolution of the feature maps (their height and width). The operation outputs the desired features \mathbf{f} specific to the bounding box \mathbf{b} out of the whole feature maps \mathbf{v} . It is crucial to emphasize that each prediction originates from a specific stride, thereby implying that its features possess the dimensionality of that specific stride. In particular, the number of channels are maintained after the *RoIAlign* operation.

Following the process outlined in the previous subsection, we obtain a collection of features $\mathbf{f}^{\varphi, c}$ for each stride φ and class c . These features are independently grouped using a clustering algorithm to yield a number $M^{\varphi, c}$ of clusters $\{\mathcal{Q}^{m, \varphi, c}\}_{m=1}^{M^{\varphi, c}}$ (line 10 of Algorithm 1). Features for each (class, stride) combination are clustered separately. The number of clusters per class can be established as a hyper-parameter, or instead determined by optimizing an internal clustering validation metric. Next, by using an aggregation function $f_{agg}(\cdot)$, we aggregate the features of all samples in each cluster, and

obtain the centroids $\mathbf{f}_{\odot}^{m,\varphi,c}$, which can be regarded as the representative of each class c and each stride φ .

Now we can define the score function $f_{OoD}(\cdot)$ of our method as shown in Eq. (1), which assigns an score to every prediction $\hat{\mathbf{y}}$ based on the features $\mathbf{f}^{\varphi,\hat{c}}$, calculated as the minimum distance $d(\cdot)$ between the features of the prediction and the centroids of the clusters of the predicted class and corresponding stride:

$$f_{OoD}(\hat{\mathbf{y}}) = \min\{d(\mathbf{f}^{\varphi,\hat{c}}, \mathbf{f}_{\odot}^{m,\varphi,c})\}_{m=1}^{M^{\varphi,\hat{c}}}. \quad (1)$$

Finally, we compute the score distribution of our ID and impose a threshold λ to determine whether a query sample is considered as ID or an OoD sample. To this end, we iterate over the ID (this time typically the validation split \mathcal{D}_{val}), obtaining the scores of all the correct predictions $\hat{\mathbf{y}}$ using the above defined score function $f_{OoD}(\hat{\mathbf{y}})$ (line **19** of Algorithm 1). This process allows computing the threshold $\lambda^{\varphi,c}$ for each class c and each stride φ to achieve the desired TPR, i.e., the percentage of ID samples inside a validation subset \mathcal{D}_{val} that will be correctly classified as ID.

At inference time, each query sample \mathbf{x}_{query} in a test dataset \mathcal{D}_{query} will be processed through the model, obtaining some predictions $\hat{\mathbf{y}}$ that will be classified as ID or OoD as:

$$\hat{\mathbf{y}} \text{ belongs to } \begin{cases} \text{ID} & \text{if } f_{OoD}(\hat{\mathbf{y}}) \leq \lambda^{\varphi,\hat{c}}, \\ \text{OoD} & \text{if } f_{OoD}(\hat{\mathbf{y}}) > \lambda^{\varphi,\hat{c}}. \end{cases} \quad (2)$$

3.3. Supervised Dimensionality Reduction

Since the algorithm operates on feature maps that come from the feature extraction part of an object detection model, it typically deals with high-dimensional features, namely, high values of D_{φ} in the previously introduced algorithm. The large dimensionality of feature maps can make feature maps become increasingly sparse due to the large volume of the feature space grows, making their distance-based characterization less effective towards detecting OoD objects.

To alleviate this effect, we propose to apply SDR techniques to the extracted features \mathbf{f} , so that FMap is able to distinguish between ID and OoD features more accurately. SDR techniques combine unsupervised dimensionality reduction algorithms with supervised loss functions to produce low-dimensional representations of the data, while preserving clear class boundaries. The SDR method can be represented as a model or trainable function

Algorithm 1: Proposed FMap detector.

Data: Training dataset \mathcal{D}_{tr} , validation dataset \mathcal{D}_{val} , query (test) dataset \mathcal{D}_{query} , number of classes C , number of strides ζ

Result: Detector ready to identify unknown objects

- 1 //Characterization of ID samples
- 2 Collect the features from correct predictions in \mathcal{D}_{tr} :
- 3 **for** $\mathbf{x} \in \mathcal{D}_{tr}$ **do**
- 4 Collect correct predictions $\hat{\mathbf{y}} \in \mathcal{Y}_{\text{correct}}$
- 5 Extract their features $\mathbf{f}^{\varphi,c} \in \mathbb{R}^{D_\varphi}$ using *RoIAlign*
- 6 **end**
- 7 **Cluster** features for each class c and each stride φ :
- 8 **for** $c \in \{1, 2, \dots, C\}$ **do**
- 9 **for** $\varphi \in \{1, 2, \dots, \zeta\}$ **do**
- 10 Obtain clusters $\{\mathcal{Q}^{m,\varphi,c}\}_{m=1}^{M^{\varphi,c}}$ with a clustering algorithm
- 11 **for** $m \in \{1, \dots, M^{\varphi,c}\}$ **do**
- 12 Compute centroids $\mathbf{f}_{\odot}^{m,\varphi,c}$ using aggregation function f_{agg}
- 13 **end**
- 14 **end**
- 15 **end**
- 16 //Computation of the thresholds
- 17 **Compute** score distribution for \mathcal{D}_{val} using Eq. (1):
- 18 **for** $\mathbf{x} \in \mathcal{D}_{val}$ **do**
- 19 Compute scores $f_{OoD}(\hat{\mathbf{y}})$ for all correct predictions
- 20 **end**
- 21 **Determine** thresholds $\lambda^{\varphi,c}$ to achieve a certain TPR over the validation set \mathcal{D}_{val} with the obtained score distribution
- 22 //Inference
- 23 **Classify** predictions $\hat{\mathbf{y}}$ from query samples $\mathbf{x}_{query} \in \mathcal{D}_{query}$ into ID or OoD using Eq. (2)

g , dependent on parameters θ , which maps the features space from dimensions \mathbb{R}^D to $\mathbb{R}^{D'}$, with $D' < D$. In the case of single-stage object detectors, as the dimensionality of the features varies depending on the stride φ , we need to train a distinct function for each stride in the object detection model. Hence, the function for the SDR method can be expressed as:

$$g_{\theta}^{\varphi}(\mathbf{f}^{\varphi}) : \mathbb{R}^{D_{\varphi}} \rightarrow \mathbb{R}^{D'_{\varphi}}. \quad (3)$$

To train parameters θ , a labeled dataset of features must be provided for each stride φ , where the labels correspond to the classes to which the features belong. In FMap, this labeled dataset is obtained during the feature collection from the ID data (lines **6** and **7** of Algorithm 1). At that stage of the FMap detector, right before creating the clusters, we can train each function g_{θ}^{φ} with those extracted features. Subsequently, we use them to transform the features to the new dimensionality, specifically $\mathbf{f}^{\varphi} \rightarrow \mathbf{f}'^{\varphi}$, where $\mathbf{f}'^{\varphi} \in \mathbb{R}^{D'_{\varphi}}$.

Once SDR has been applied over the feature maps, the FMap detector operates as described in Algorithm 1, with the key difference that each time the features of a prediction are extracted, they are transformed to the new dimensionality using the corresponding function $g_{\theta}^{\varphi}(\mathbf{f}^{\varphi})$. This process occurs in lines **19** and **23** of Algorithm 1.

3.4. Enhanced Unknown Object Localization

One key aspect of the usage of OoD techniques for unknown object detection is their reliance on the predictions generated by the single-stage model, which in turn depend on the inference confidence threshold, a user-selected hyperparameter. The inference confidence threshold represents the minimum confidence value a prediction must achieve to be considered valid and subsequently be output by the model. Specifically, these OoD methods can only identify an unknown object if it has been incorrectly predicted as one of the known classes, at which point the algorithm must detect this prediction as an OoD instance or unknown object. Hence, the inference confidence threshold controls the relation between the precision in detecting known objects and the recall of unknown objects: lowering its value would probably result in more unknown objects detected, but at the penalty of increasing the missed classifications of known objects.

To reduce this dependency, we propose an unsupervised algorithm to generate proposals for potential unknown objects regardless of the inference

confidence threshold, i.e., to improve the unknown recall of the FMap detector. This additional algorithm, hereafter referred to as *Enhanced Unknown object Localization* (EUL), hinges on the hypothesis that high-resolution feature maps may contain information about unknown objects that the model does not ultimately output as predictions. The overall workflow of EUL is as follows, whose steps are illustrated in Figure 2 with numbers therein linked to the ones below:

- ① *High resolution feature map extraction*: To accurately locate possible unknown objects in the image, we extract the feature maps from the stride $\varphi \in \{1, \dots, \zeta\}$ corresponding to the highest resolution.
- ② *Feature map information aggregation*: we next condense the information from all channels of the feature maps to yield a saliency map, i.e., an image with the same resolution but only one channel, which highlights areas of the image that, in this case, likely contain objects.
- ③ *Saliency map binarization*: the saliency map is converted into a binary format. This involves setting a threshold value, such that pixels with saliency values above this threshold are set to 1 (indicating potential object presence), while those below the threshold are set to 0 (indicating background). Multiple thresholds can be selected in order to obtain several binarized images to search for objects of different sizes. The selection of the thresholds can be done manually as a hyperparameter, or automatically tuned by resorting to methods like Otsu thresholding [28].
- ④ *Region and bounding box calculation*: After applying the threshold(s), EUL utilizes connected-component labeling to identify contiguous regions, each representing a potential object in the original image. For each of these regions, we compute the bounding box surrounding the region at hand by finding the minimum and maximum coordinates within each connected component. Since the bounding boxes are calculated at the spatial resolution of a feature map, they need to be rescaled to the original image size.
- ⑤ *Filtering by ranking*: The previous operations generate a large number of proposals; the meaningful ones are retained by using a ranking method and by selecting the top-k best proposals. To this end, features of all these proposals are first extracted through the *RoIAlign* operation. Subsequently, for each class, the minimum distance between these features

and the clusters of the class are computed. It is important to remark that the utilized stride is the one with the highest resolution, as previously discussed. Hence, each feature is associated to a vector with the minimum distance to each class. These distances are then consolidated into a single metric by computing the entropy of a vector of pseudo-probabilities built from such distances, which quantifies how far the feature vector is from the representative of all classes within the stride with largest resolution. If we denote the distances as $\{d_1, d_2, \dots, d_C\}$, the computed entropy is given by:

$$H(\hat{\mathbf{b}}) = - \sum_{c=1}^C d_c^* \log_C d_c^*, \quad (4)$$

where $d_c^* = d_c / \sum_{c=1}^C d_c$, and $H(\hat{\mathbf{b}}) = 1$ if $d_c = 1/C \forall c \in \{1, \dots, C\}$. As a result, each bounding box is ranked by a single entropy value computed on its features. Proposals exhibiting the lowest entropy are preferentially retained, based on the hypothesis that lower entropy values correlate with a higher probability of identifying a genuine object.

4. Experimental Setup

In order to assess the performance of the proposed FMap detector, we design an extensive experimentation aimed to inform the responses to four research questions (RQ), formulated as follows:

- RQ1: Which is the optimal configuration for the proposed FMap OoD detector?
- RQ2: How does FMap perform when compared to logits-based post-hoc OoD detection methods in single-stage object detectors?
- RQ3: Does a fusion of feature-based methods with logits-based methods outperform other potential ensemble configurations?
- RQ4: How do unknown object detection algorithms implemented on single-stage models perform when compared to the state of the art?

The remainder of this section offer details on the benchmark (Subsection 4.1, evaluation metrics (Subsection 4.2), implementation details (Subsection 4.3), post-hoc methods for comparison (Subsection 4.4) and fusion strategies

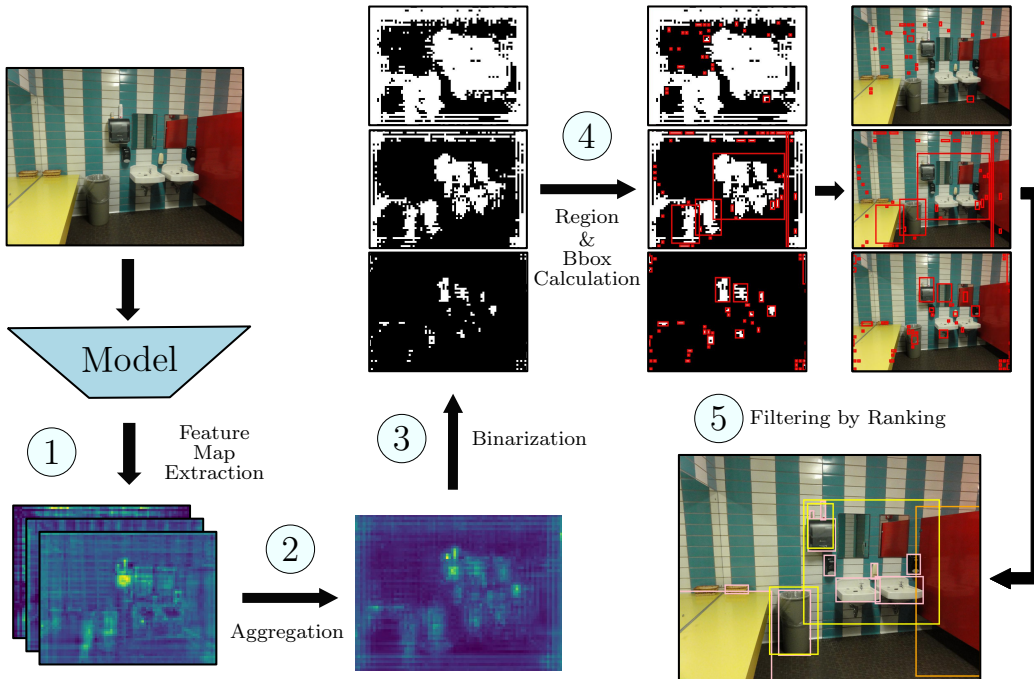


Figure 2: Graphical example of the application of the Enhanced Unknown Localization (EUL) algorithm. Red boxes in step ④ are bounding box proposals. In the final image after step ⑤, the orange box is an unknown object detected by the basic FMap algorithm, whereas yellow are the boxes selected by EUL, and finally the pink boxes are the unknown object annotations.

(Subsection 4.5), all under consideration for the experiments reported in the manuscript. For the sake of replicability and to foster follow-up studies, scripts and results have been made in a public GitHub repository available at: https://github.com/aitor-martinez-seras/OoD_in_Object_Detection.git.

4.1. Evaluation Benchmark

The evaluation is based on the UOD benchmark presented in [25]. It follows the practice of previous works on the topic of open-world object detection by using the PASCAL VOC dataset [20] as the training ID dataset, which contains annotations of 20 object categories. For test purposes, the UOD benchmark uses two subsets of the COCO dataset [21], namely COCO-OoD and COCO-Mix. The former contains only objects that are unknown, whereas the latter mixes both known and unknown instances. In both cases, un-

knowns are instances of the other 60 classes contained in **COCO**, jointly with new unknown instances labeled by [25], with images being handpicked. More details of this benchmark can be found in their paper. The number of known and unknown objects are shown in Table 1. This benchmark is used in the experiments of all research questions formulated above.

Dataset		Number classes (total/known/unknown)	Number of images	Known objects	Unknown objects
ID	Pascal VOC	20/20/0	11,530	27,450	-
OoD	COCO-OoD	60+1/0/60+1	504	-	1,655
OoD	COCO-Mix	80+1/20/60+1	897	2,533	2,658

Table 1: Number of images and annotated known and unknown objects per subset in the UOD benchmark. The ‘+1’ in the **COCO-OoD** and **COCO-Mix** datasets refer to the additional class defined by the authors of [25] to collectively refer to newly annotated unknown objects over the original **COCO** dataset.

4.2. Evaluation Metrics

To gauge the performance of the models in detecting known and unknown objects, we consider several metrics widely used in the literature related to this area [25]. To evaluate the performance of known object detection we consider the mean Average Precision (mAP) considering that an object is spatially detected in the image when the IoU between a bounding box prediction and the true bounding box of the object is at least 0.5. In order to evaluate the performance in OoD or unknown object detection, we first define TP_u as the true positive proposals of unknown objects (i.e., correctly detected unknowns); FN_u for false negative proposals (namely, unknowns detected as knowns), and FP_u for false positive proposals (corr. known objects detected as unknown). Based on these definitions, we utilize the following performance metrics:

- The Unknown Average Precision (U-AP), the average precision computed only over the unknown class.
- The Recall Rate (U-REC) and Precision Rate of Unknown objects (U-PRE), defined as:

$$\text{U-REC} = \frac{TP_u}{TP_u + FN_u}, \quad \text{U-PRE} = \frac{TP_u}{TP_u + FP_u}. \quad (5)$$

- The Unknown F1-Score defined as the harmonic mean of U-PRE and U-REC, given by:

$$\text{U-F1} = \frac{2 \cdot \text{U-PRE} \cdot \text{U-REC}}{\text{U-PRE} + \text{U-REC}}. \quad (6)$$

- The Absolute Open-Set Error (A-OSE), by [29], employed to report the count of unknown objects that are wrongly classified as any of the known classes.
- The Wilderness Impact (WI) metric, defined in [19] as:

$$\text{WI} = \frac{\text{Precision in closed-set}}{\text{Precision in open-set}} - 1, \quad (7)$$

which is used also to characterize the case that unknown objects are confused with known objects.

4.3. Implementation Details

In terms of software implementation, we rely on the model templates provided by the Ultralytics library [30], selecting YOLOv8 as the one-stage object detector used throughout the experiments. The number of strides ζ is 3. We trained the model from scratch over the PASCAL VOC ID training dataset for 300 epochs, using a batch size equal to 16.

RoIAlign and aggregation operations. We use average as the operation to perform the aggregation of the features $f_{agg}(\cdot)$ in the vanilla FMap method. For *RoIAlign*, it is necessary to choose the height and width of the resulting features. We opt for a one-pixel (1×1) output size, hence every prediction’s features will be of size equal to the number of channels in the corresponding stride.

Determining the thresholds for the OoD methods. FMap requires determining a threshold for each class and stride. Therefore, we need sufficient samples in each case for the thresholds to be representative of the ID data. Therefore, instead of only using the validation split from the training dataset (PASCAL VOC in this case), we harness all samples within the train and validation datasets to compute these thresholds. Furthermore, the TPR used to determine the thresholds $\lambda^{\varphi,c}$ is set at 95%, which is a common choice in the literature.

Distance metrics. The scoring function of FMap $f_{OoD}(\cdot)$ uses a distance computation to assess the dissimilarity between features. To evaluate different options for this distance we will consider L_1 , L_2 and *cosine* distances for the purpose.

Clustering algorithms. FMap can be combined with any clustering technique, so we have tested a few in this research, namely *KMeans* and *HDBSCAN*. To optimize them, we make a grid search of their different hyperparameters, and select the configuration that attains the best Silhouette score, individually for each class in each stride. For the case of *KMeans*, as the optimization algorithm tends to create 2 to 3 clusters in each case, we have also tested to force the algorithm to create 10 clusters. In addition, we include the case where all data is assumed to belong to a single, large cluster, denoting this case as *One*.

Supervised dimensionality reduction. To implement SDR, we have chosen the *IVIS* framework presented in [31]. Essentially, the technique works by utilizing a Siamese network architecture trained by a variant of the standard triplet loss. After a grid search, the selected hyperparameter values are an output embedding dimension of 32 ($D'_\varphi = 32$) and a k value of 15, which controls the number of nearest neighbors to retrieve for each point. The same output dimension is selected for the three strides. We refer to [31] for more details of the inner workings of *IVIS*.

Enhanced unknown object localization. For the feature map aggregation, we compute the mean absolute deviation. For the binarization, a fast variation of the recursive Otsu thresholding method [28] is used.

4.4. Post-hoc OoD Detection Methods

The post-hoc OoD detection methods implemented for our experimental benchmark are selected based on their model-agnostic nature, i.e. they can be directly applicable to any type of classification branch within a neural network model, without any ambiguity of how they should be implemented.

Post-hoc techniques like MSP [12], Energy [14] and ODIN [13], which only rely on the output of a classification branch, meet the criteria of being directly applicable to a one-stage object detector. We refer to them as *logits-based methods*, as they only operate on the logits of the classification branch to compute their OoD scores. These three mentioned methods are the ones included in our benchmark. In case of ODIN, the input perturbation is

not applied as it is not clear how it should be implemented when multiple predictions can be issued per every image.

It is important to note that the YOLOv8 model does not produce a vector of class probabilities for each bounding box prediction. Instead, it outputs a vector of class “confidence” values, obtained by applying the sigmoid activation function in the final layer. For the purposes of this study, we have used the raw output of this final layer, prior to the application of the sigmoid activation function, as the model’s internal information used by the implemented post-hoc techniques to elicit their OoD scores.

4.5. Fusion Strategies

In response to RQ3, we investigate the performance of ensembles of feature-based (like the proposed FMap) and logits-based OoD techniques. The fusion of FMap with the considered post-hoc algorithms finds its motivation in the results of [9], where fusion strategies were also explored for detecting OoD instances in image classification tasks.

When fusing two OoD techniques, it is crucial to establish a criterion to resolve discrepancies between the predictions of both methods. One option can be to employ an AND criterion, by which a sample is declared to be OoD if both methods classifies it as such. This approach typically results in increased precision (U-PRE) but decreased recall (U-REC) for unknown objects. In contrast, an OR criterion would yield a sample classified as OoD if any of the methods (or both of them) predicts the sample as such. Consequently, an OR fusion rule potentially increases the recall at the expense of precision for both known and unknown objects. Figure 3 summarizes the operational mechanics of the AND and OR voting strategies.

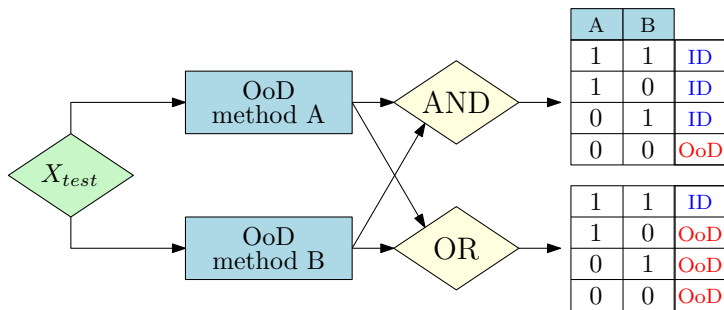


Figure 3: Illustration of the AND and OR fusion strategies. A decision of ‘1’ indicates that the method identifies the prediction as ID, whereas ‘0’ indicates the contrary.

With the goal of balancing precision and recall, we propose a soft voting strategy coined as SCORE. This strategy requires that each method to be fused computes a fusion score via a designated fusion function, $f_{fusion}(\cdot)$. This score quantifies the extent to which a sample is considered ID, based on the deviation of the OoD score for a given OoD technique from the corresponding threshold. The fusion score ranges from -1 to 1, where 1 signifies a strong likelihood of the sample being ID, and -1 indicates a strong likelihood of the sample being OoD. These scores are aggregated to produce a final fusion score that determines the sample’s classification:

$$f_{fusion}(\hat{\mathbf{y}}) = f_{OoD}^A(\hat{\mathbf{y}}) + f_{OoD}^B(\hat{\mathbf{y}}), \quad (8)$$

$$\hat{\mathbf{y}} \text{ is classified as } \begin{cases} \text{ID} & \text{if } f_{fusion}(\hat{\mathbf{y}}) > 0, \\ \text{OoD} & \text{if } f_{fusion}(\hat{\mathbf{y}}) \leq 0, \end{cases} \quad (9)$$

where superscripts A and B represent the scores from the OoD methods A and B that are fused together.

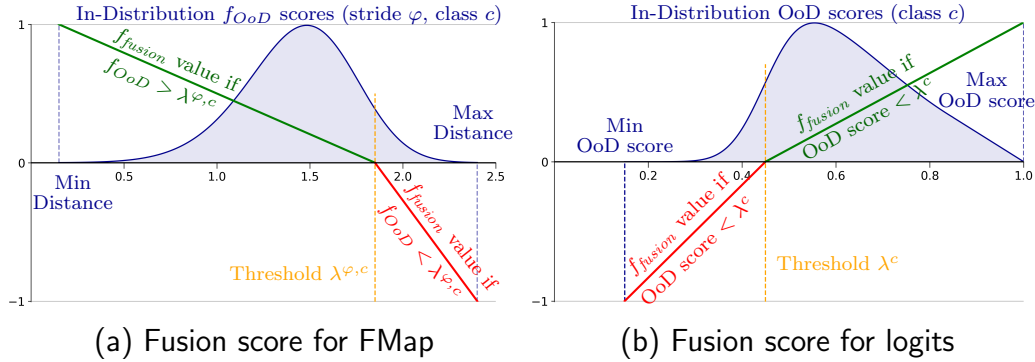


Figure 4: Example of the application of the SCORE strategy. Each method computes a fusion score for $f_{fusion}(\cdot)$ using the piece-wise functions depicted in green and red. Values outside the defined range are clipped to the minimum and maximum values, respectively.

Figure 4 illustrates the calculation of the fusion score for feature maps and logits-based methods. The process involves collating the minimum and maximum ID values, which subsequently define the boundaries of the piece-wise function $f_{fusion}(\cdot)$. Depending on whether the OoD score for a particular method falls below or above the threshold, the corresponding segment of the piece-wise function is utilized to compute the fusion score.

5. Results and Analysis

We now proceed by presenting and discussing on the experimental results obtained to address the RQs posed in the previous section. First, we aim to determine which FMap configuration performs best (RQ1, Subsection 5.2). Then, we compare FMap to existing post-hoc methods (RQ2, Subsection 5.3). Subsequently, we combine FMap with post-hoc methods to ascertain if the resulting ensemble of feature-based and logits-based methods elicits better results than when used separately (RQ3, Subsection 5.4). Finally, we compare our findings against state-of-the-art OoD detection methods designed for object detection models (RQ4, Subsection 5.5).

5.1. Preamble

Since this paper gravitates on single-stage object detection models with open-world detection capabilities, we focus on finding the optimal configuration of the selected YOLOv8 object detector by balancing the performance in detecting both known and unknown objects. Hence, we focus on mAP as the representative score quantifying the capability of the model to detect known instances, whereas U-F1 is the indicator of the method’s effectiveness in recognizing unknown objects. Specifically, for the latter we use the sum of unknown F1 (hereafter referred to as U-F1 in the text and $U-F1_{SUM}$ in the plots) obtained on both `COCO-OoD` and `COCO-Mix`, while mAP is calculated only from `COCO-Mix` since `COCO-OoD` includes only annotations for unknowns objects.

Building on these methodological choices, it is important to highlight the insight presented in Subsection 3.4, where we emphasize the significance of the inference confidence threshold. This threshold can be regarded as a variable that calibrates the balance between the model’s known and unknown object detection capabilities. Thus, during the performance assessment of the single-stage model (RQ1, RQ2 and RQ3), we aim to delineate the trade-off between known and unknown detection metrics arising when configuring the inference confidence threshold. We represent this trade-off by means of two-dimensional scatter plots, with the different configurations of cluster methods and distance metrics distinguished by unique markers and colors. For each configuration, several inference confidence thresholds are tested and plotted. The optimal configurations are those which are non-dominated by any other configuration/technique (in the Pareto sense), i.e. those for which there is no other configuration/technique that improves one objective without worsening

the other. Non-dominated configurations/techniques are highlighted with red circles and connected by a red dashed line. Additionally, their A-OSE values are displayed alongside each red circle. Finally, results of all metrics of the best configurations for every research question are given in Appendix A.

5.2. RQ1: Which is the optimal configuration for FMap?

To address this first research question, we identify the non-dominated configurations for the FMap method for its naive (*vanilla*) version (Algorithm 1), and when expanded with the SDR (Subsection 3.3) and EUL (Subsection 3.4) techniques. Subsequently, we compare these optimal configurations to delineate the final front of non-dominated FMap configurations.

Vanilla FMap. The initial analysis involves the vanilla version of the FMap method, examined in conjunction with various clustering methods and distance metrics. The comparative results are depicted in Figure 5. A first glance at this plot verifies that the choice of clustering method (indicated by color) significantly impacts on the performance of the model in detecting known objects (mAP). Generally, aggregating all features into a single large cluster per class and stride (denoted as the *One* cluster method, shown in blue) results in higher mAP and lower U-F1 scores. Conversely, configurations that generate multiple clusters (thereby increasing the number of centroids for comparison) typically exhibit reduced mAP scores, but enhanced performance in detecting unknown objects. Notably, increasing the number of clusters from 2 to 3 – which often occurs in our experiments with both *KMeans* (in red) and *HDBSCAN* (in orange) – to forcing 10 clusters in *KMeans* (denoted as *KMeans*¹⁰, in green) leads to a further decrease in mAP while marginally improving U-F1. These observations are corroborated by examining the non-dominated configurations. Configurations yielding the highest mAP predominantly utilize the *One* clustering method, while those achieving larger U-F1 scores generally employ a greater number of clusters. Notably, the best U-F1 score is achieved using *KMeans*¹⁰. Furthermore, with respect to the A-OSE metric (which quantifies the number of unknown instances erroneously classified as known objects) the depicted results expose a clear trend: an increase in the number of clusters correlates with a reduction in classification errors for unknown instances, i.e., lower A-OSE values.

Additionally, an analysis of the impact of distance metrics reveals significant findings. The L_1 and L_2 distance metrics typically enhance the detection

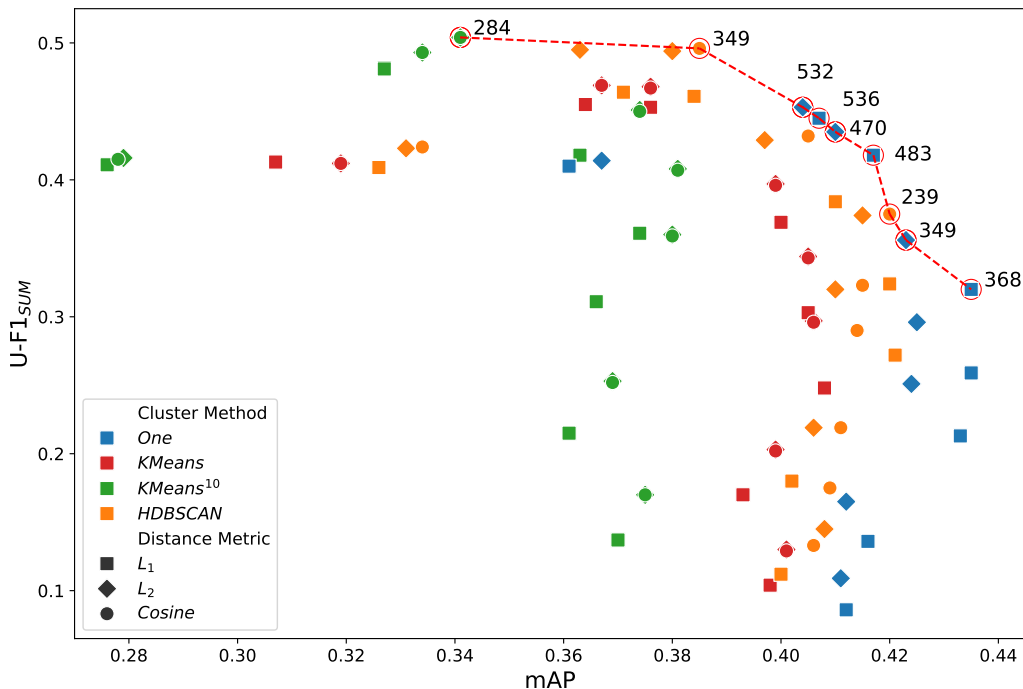


Figure 5: Front of non-dominated FMap configurations in the mAP versus U-F1_{SUM} trade-off for the vanilla version of FMap. Points correspond to different configurations of the model in terms of distance metrics (represented by marker types) and clustering methods (indicated by color). For each configuration, various inference confidence thresholds are represented. We refer to Subsection 5.1 for further details.

of known objects, while not providing major differences between them. Conversely, the *Cosine* distance metric demonstrates superior performance in terms of robustness and the recognition of unknown objects, as evidenced by improved A-OSE and U-F1 scores, respectively.

FMap with SDR. We next apply SDR to FMap to lower the dimensions of the features before their characterization via the clustering methods under consideration. Figure 6 summarizes the results, from which similar insights concerning the impact on performance of distance metrics and clustering methods can be drawn. In general, the *Cosine* distance and a high number of clusters correlates with larger U-F1 scores. In contrast, using L_1 and L_2 metrics and only one cluster leads to increased known object performance, and slightly reduced U-F1 scores. Another key finding is that the robustness provided by the use of *Cosine* distance in reducing the unknown objects

wrongly classified as known classes – lowering the A-OSE metric – becomes even more apparent when utilizing SDR within FMap.

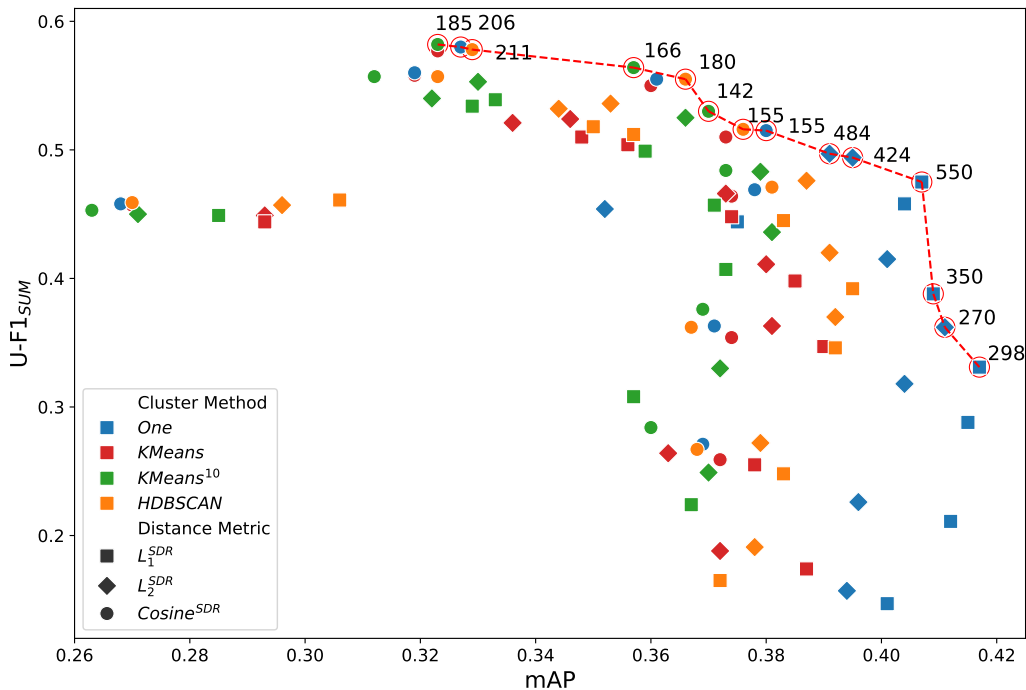


Figure 6: Front of non-dominated FMap configurations in the mAP versus $U-F1_{SUM}$ trade-off for FMap with SDR. Points correspond to different configurations of the model in terms of distance metrics (represented by marker types) and clustering methods (indicated by color). For each configuration, various inference confidence thresholds are represented.

FMap with EUL. Now we apply the EUL algorithm presented in Subsection 3.4 to boost the unknown localization capabilities of the one-stage object detector. Consistently with earlier results, Figure 7 illustrates that the *Cosine* distance, when paired with a clustering technique that generates more than one cluster, consistently achieves the best U-F1 scores. Meanwhile, the highest mAP is obtained using the L_2 metric with a single cluster. Nevertheless, in this scenario, the variability in unknown detection performance (U-F1) between the worst and best methods among the non-dominated ones is significantly smaller, narrowing from 18% with vanilla implementation and 25% when SDR is applied, to merely 5% under the EUL configuration. In contrast, the performance disparity in detecting known objects (mAP) remains

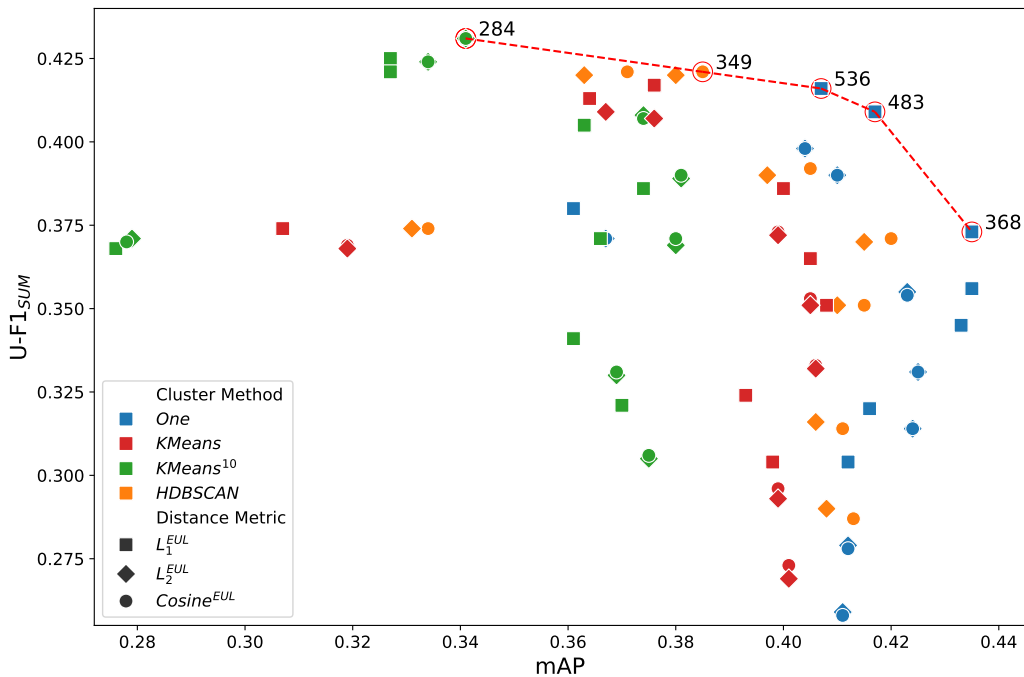


Figure 7: Front of non-dominated FMap configurations in the mAP versus $U-F1_{SUM}$ trade-off for FMap with EUL. Points correspond to different configurations of the model in terms of distance metrics (represented by marker types) and clustering methods (indicated by color). For each configuration, various inference confidence thresholds are represented.

consistent across all three scenarios.

Comparison. Lastly, we evaluate the optimal combinations of cluster method, distance metric, and inference confidence threshold across all three versions of the algorithm (the non-dominated configurations from the vanilla FMap, FMap with SDR and FMap with EUL). This comparative analysis is depicted in Figure 8. Results therein depicted clearly demonstrate a general trend: the FMap method enhanced with SDR consistently excels at detecting unknown objects, also achieving excellent A-OSE values when compared to other configurations. Conversely, the vanilla FMap detector maintains the original known object detection capabilities more effectively, while delivering reasonable U-F1 scores. Finally, the addition of EUL is only beneficial when the specific combination of cluster method, distance metric and confidence threshold yields high mAP values, but low U-F1 scores. In such scenarios, EUL is capable of enhancing the unknown detection capabilities without

sacrificing the mAP performance.

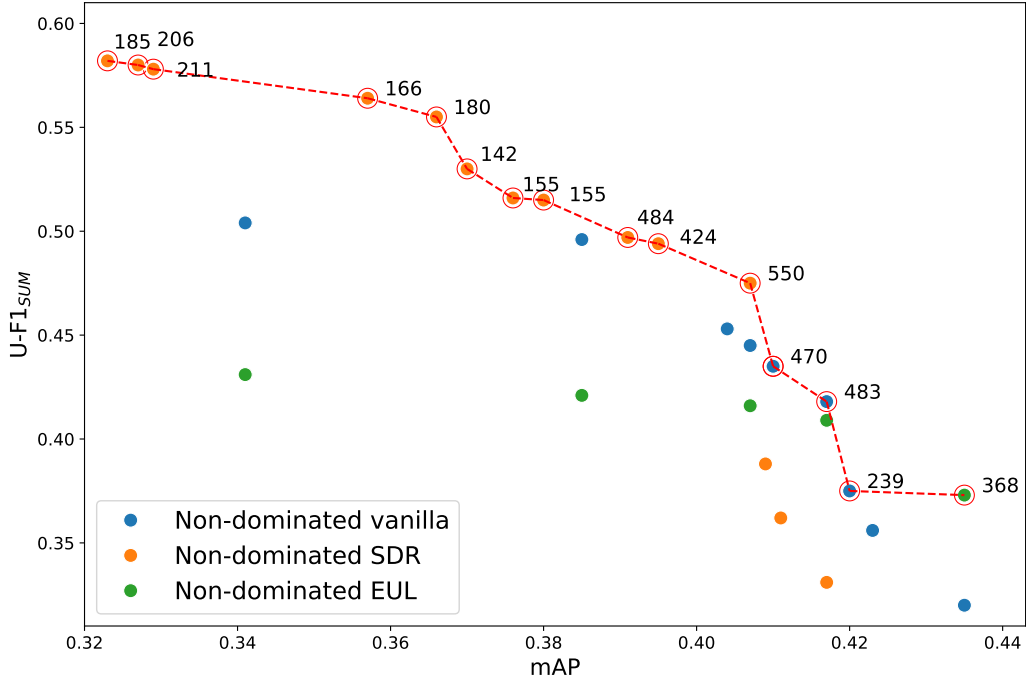


Figure 8: mAP and $U-F1_{SUM}$ pareto front for non-dominated FMap parameter combinations of the three versions of the algorithm (vanilla, SDR and EUL).

Nonetheless, we note that EUL technique focuses on improving the recall of unknown objects. Its application, however, causes a decrease in precision finally leading to lower U-F1 scores. Hence, it is interesting to inspect the precision-recall trade-off in unknown object detection for these non-dominated solutions. This detailed analysis is presented in Figure 9, clearly revealing that EUL sacrifices precision for recall in unknown objects.

In conclusion, each version of the algorithm assessed in response to RQ1 exhibits distinct strengths and weaknesses. On the one hand, using SDR provides superior unknown detection capabilities and robustness while maintaining an acceptable known detection performance. On the other hand, EUL significantly boosts the recall of the vanilla FMap when detecting unknown objects, at the cost of considerably reducing the precision in most of the cases, hence obtaining lower U-F1 scores. Nevertheless, EUL manages to enhance the U-F1 of the vanilla FMap to a degree that it becomes one of the non-dominated parameter configurations. Finally, configurations of the

vanilla FMap obtain an acceptable balance between mAP and U-F1, overriding the computational overhead associated with the other two versions under consideration. As a concluding note, in all cases L_1 and L_2 metrics perform similarly, so hereafter we will focus only on L_1 .

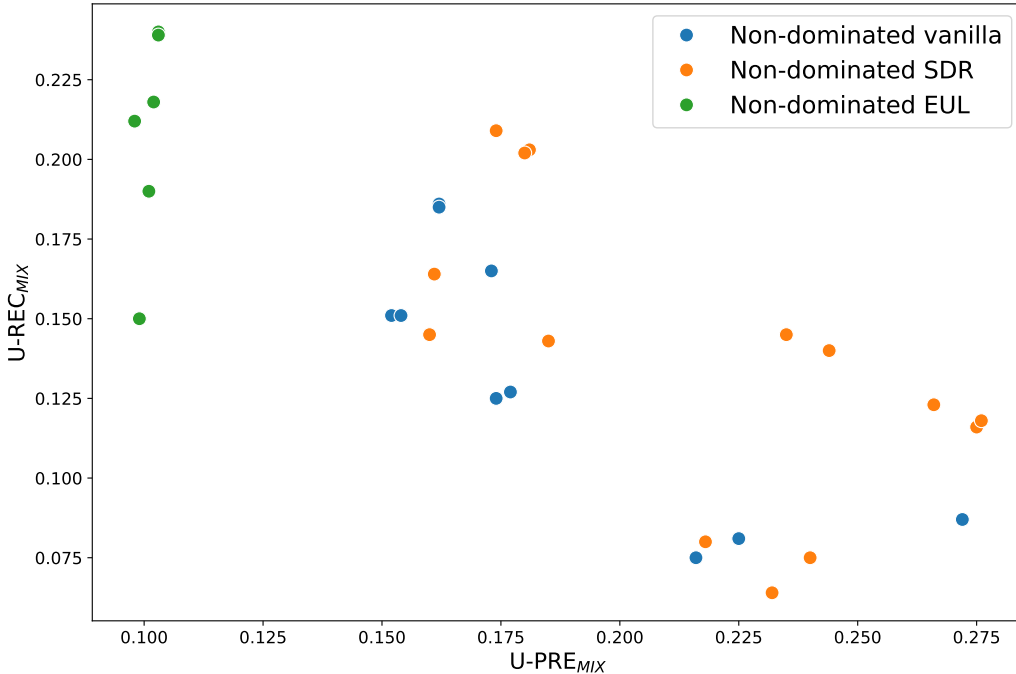


Figure 9: Precision vs Recall in COCO-Mix subset of non-dominated FMap parameter combinations for the three versions of the algorithm (vanilla, SDR and EUL).

5.3. RQ2: How does FMap perform when compared to logits-based post-hoc OoD detection methods in single-stage object detectors?

Our discussion follows by evaluating the performance of the optimal configurations of FMap found in the previous section, and by comparing it to that of post-hoc or logits-based techniques. These methods also depend on the inference confidence threshold set for the single-stage object detector, prompting the testing of several confidence thresholds for each post-hoc algorithm.

The results of this performance comparison are depicted in Figure 10. Among the post-hoc methods, MSP emerges as the top performing one. When compared to the FMap method at comparable levels of unknown F1

score, post-hoc methods generally maintain better known object detection capabilities. However, the SDR version of FMap surpasses the U-F1 score of the MSP method, though this comes with a reduction in mean average precision. Summarizing, the post-hoc methods achieve similar U-F1 scores when compared to our technique while maintaining remarkable performance over the known classes.

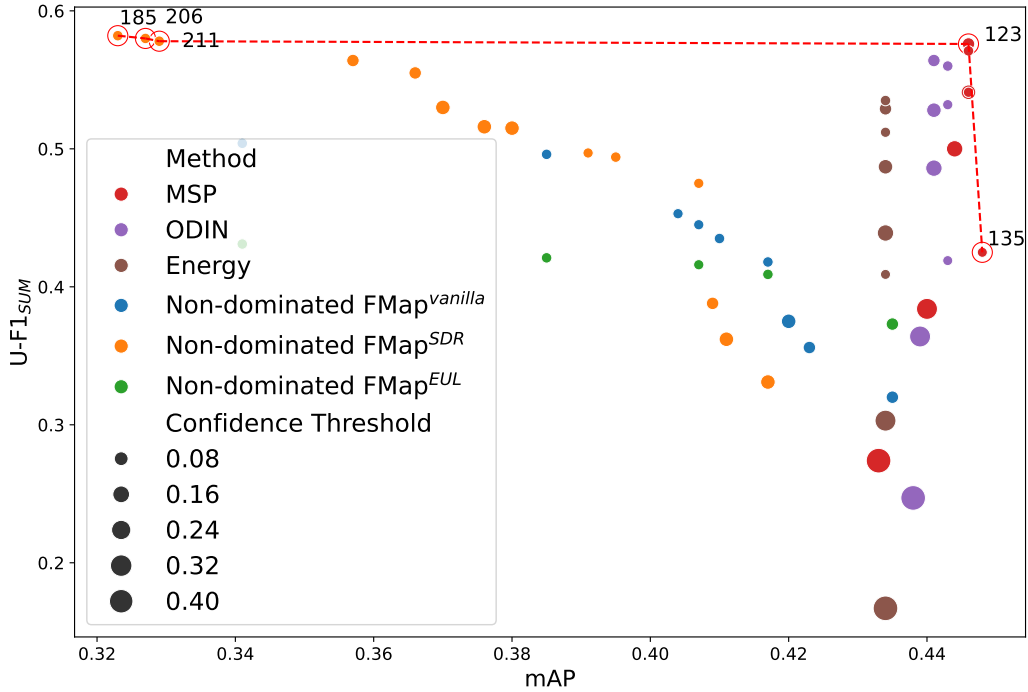


Figure 10: Non-dominated parameter combinations of the three versions of the algorithm (vanilla FMap, FMap with SDR and FMap with EUL) against post-hoc logits-based techniques.

5.4. RQ3: Does a fusion of feature-based methods with logits-based methods outperform other potential ensemble configurations?

The results achieved in response to RQ2 suggest an important question. Although the FMap method is marginally outperformed by post-hoc detection techniques, could it potentially serve as a superior choice for method fusion, as opposed to relying solely on the more effective logits-based methods for ensemble strategies?

To verify this hypothesis, which lies at the core of RQ3, we have first tested several possible ensembles together with the different fusion strategies defined in Subsection 4.5. Figure 11 presents the results of this prior study, where the distance metric used in the FMap method is used to name the fusion of methods. It can be clearly seen that the OR criterion (in blue) provides the best U-F1 values in exchange for known object detection capabilities, whereas the AND strategy (in orange) behaves conversely. As stated, the SCORE criterion (in green) establishes a balance in the trade-off between both metrics. Nevertheless, only one of the ensembles of this strategy is a non-dominated one. The other fusion ensemble contributing to the set of non-dominated configurations are combinations of MSP with either another post-hoc method or a feature-based technique (FMap). The fusion of different well-performing versions of FMap does not give rise to any non-dominated solution.

To allow for a better visualization of the final results of RQ3, we have grouped together the different ensembles attending to the type (feature- or logits-based) of the fused methods. Additionally, we compare them to the techniques previously selected in RQ1 and RQ2. This is graphically depicted in Figure 12. We can extract valuable insights from this plot. On one hand, FMap (in blue) obtains remarkable unknown object detection capabilities for some of the configurations, but it alone can not outperform the rest the techniques when accounting for both mAP and U-F1. On the other hand, the most successful post-hoc technique, MSP, becomes part of the global set of non-dominated configurations/ensembles. In fact, it yields very similar performance to the combination of two post-hoc or logits-based methods. Finally, the combination of FMap with the best logits-based approaches (MSP) achieves the best U-F1 score for one on the possible configurations, while scoring also a superior known object detection performance in other configurations.

In conclusion, the results provided to answer RQ3 verify that the fusion two of post-hoc logit-based methods attain very similar performance in both known and unknown object detection when compared to the method alone. Conversely, fusing a feature-based method (FMap) with post-hoc detection methods ensures synergistically diverse decisions, ultimately leading to a more robust OoD detection performance. Therefore, we can confidently assure that the fusion of feature-based methods with logits-based methods outperform other fusion possibilities. Moreover, the best fusion configurations attain better results than state-of-the-art methods, as evinced by the

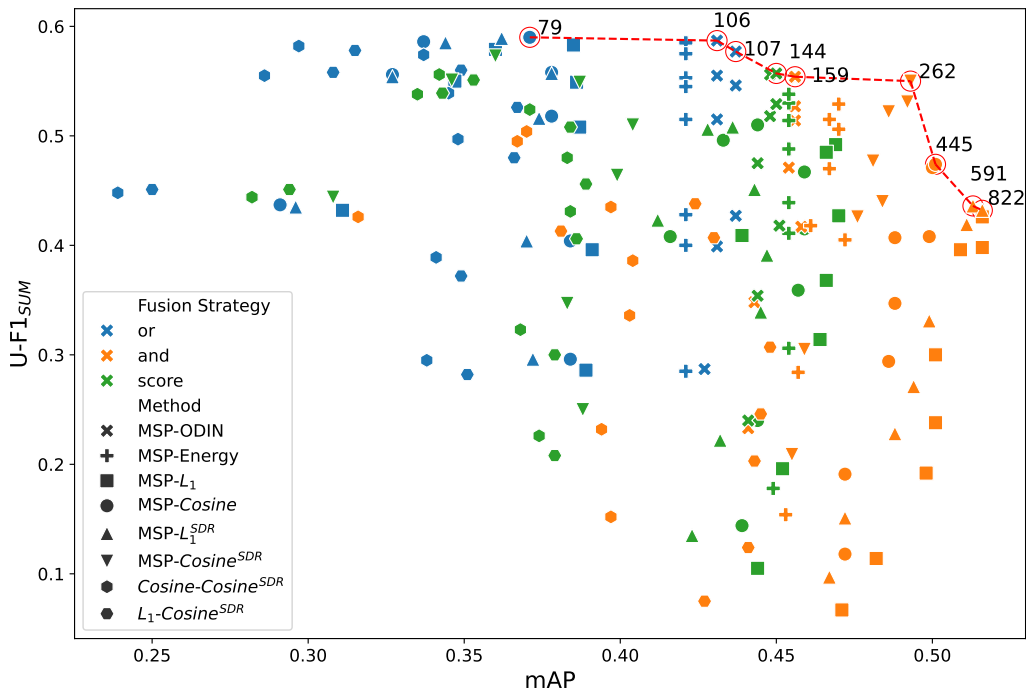


Figure 11: mAP and $U-F1_{SUM}$ scores across various fusion possibilities of detection methods, distinguished by marker style, and for the three different fusion strategies, indicated by color. The naming convention is $Method_A$ - $Method_B$, whereas the inclusion of FMap in the fusion ensemble is denoted by the distance metric in use: L_1 , L_1^{SDR} , $Cosine$ and $Cosine^{SDR}$.

metrics provided in the caption of Figure 12 (not included in the plot for the sake of readability). This is further analyzed in our discussion around RQ4.

5.5. RQ4. How does the performance of unknown object detection algorithms implemented on single-stage models compare to that of the SOTA?

We conclude our experiments with RQ4, for which we compare the best performing FMap-based methods discovered so far to state-of-the-art methods in the UOD benchmark [25]. For the sake of readability in the reported results, we have selected the most recent and well-performing comparison baselines, and we have also included the most competitive results of the vanilla, SDR and EUL versions of FMap.

Results are presented in Table 2. When examining the detection outcomes for known objects, it becomes evident that the mAP values for the

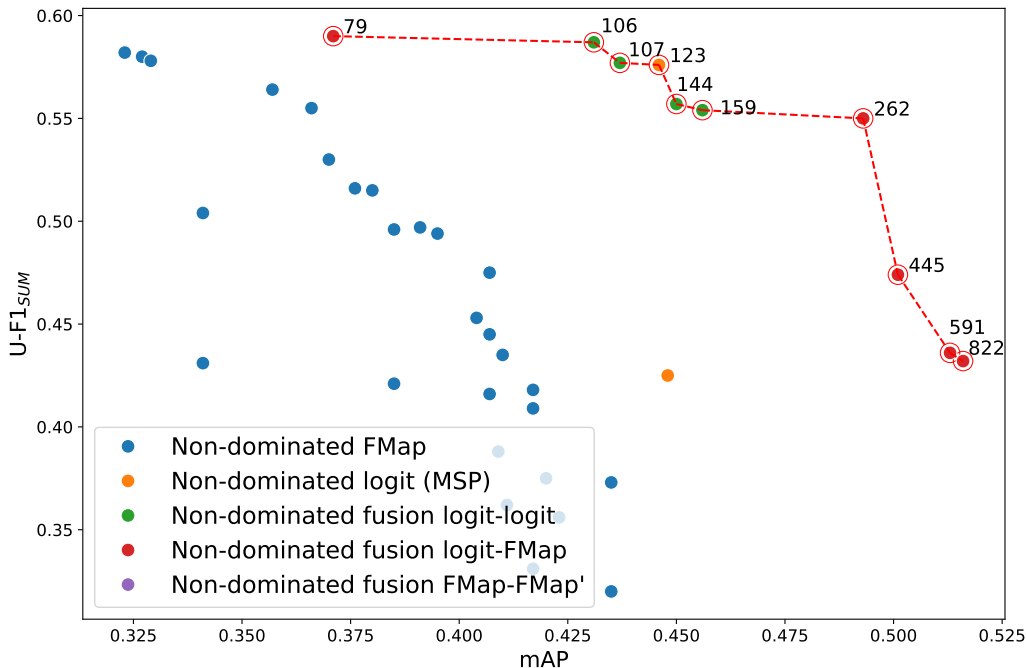


Figure 12: mAP versus $U-F1_{SUM}$ across the best feature-based (FMap), logit-based (post-hoc) and fusion types. The fusion of different parameter combinations of FMap does not yield any non-dominated solution compared to the other ensembles, hence they do not appear in the plot. For reference, VOS² [15] reaches 0.36 mAP and 0.49 $U-F1_{SUM}$, ORE [5] reaches 0.21 mAP and 0.43 $U-F1_{SUM}$ and UnSniffer [25] reaches 0.36 mAP and 0.77 $U-F1_{SUM}$.

single-stage YOLOv8 model consistently surpass those achieved by Faster R-CNN and DETR. Additionally, it is noteworthy that YOLOv8 methods exhibit generally higher precision for unknown objects. However, these methods often achieve lower recall rates, which contributes to a more balanced U-F1. Subsequently, the highest U-F1 is achieved by UnSniffer. As for the rest, FMap-based methods demonstrate enhanced robustness, as evidenced by consistently achieving lower scores in both A-OSE and WI metrics, indicative of a reduced propensity to misclassifying unknown objects as known. This robustness is attributed to our approach, as it avoids any need for specialized retraining (contrary to state-of-the-art methods, which require retraining the object detector with pseudo-labels for identifying unknown classes), significantly diminishing the likelihood of such misclassifications.

Method	Base Model	VOC-test					COCO-OoD					COCO-Mix				
		mAP	U-AP	U-F1	U-PRE	U-REC	mAP	U-AP	U-F1	U-PRE	U-REC	A-OSE	WI			
-		0.483	-	-	-	-	-	-	-	-	-	-	-			
MSP		0.470	0.213	0.314	0.279	0.359	0.364	0.055	0.169	0.190	0.153	588	0.135			
Mahalanobis		0.447	0.129	0.271	0.309	0.241	0.351	0.051	0.149	0.207	0.116	604	0.165			
Energy score	Faster	0.474	0.213	0.308	0.260	0.377	0.364	0.048	0.169	0.167	0.171	470	0.137			
ORE	R-CNN	0.243	0.214	0.255	0.153	0.782	0.213	0.140	0.175	0.103	0.592	485	0.089			
VOS ¹		0.485	0.135	0.196	0.342	0.137	0.377	0.040	0.101	0.262	0.062	640	0.152			
VOS ²		0.469	0.205	0.317	0.291	0.348	0.364	0.051	0.172	0.184	0.163	409	0.124			
UnSniffer		0.464	0.454	0.479	0.433	0.535	0.359	0.150	0.287	0.222	0.409	398	0.175			
OW-DETR	DETR	0.420	0.033	0.056	0.030	0.380	0.414	0.007	0.025	0.014	0.161	569	0.086			
-		0.750	-	-	-	-	-	-	-	-	-	-	-			
<i>Cosine</i>		0.620	0.160	0.243	0.655	0.149	0.420	0.025	0.132	0.272	0.087	239	0.120			
<i>Cosine</i> ^{SDR}		0.471	0.296	0.392	0.427	0.363	0.323	0.061	0.190	0.174	0.209	185	0.082			
<i>Cosine</i> ^{SDR}		0.527	0.238	0.351	0.668	0.238	0.380	0.051	0.164	0.275	0.116	155	0.087			
L_1^{EUL}	YOLOv8	0.662	0.161	0.254	0.239	0.270	0.435	0.031	0.119	0.099	0.150	368	0.141			
MSP		0.719	0.237	0.390	0.565	0.298	0.446	0.083	0.186	0.237	0.153	123	0.073			
MSP- <i>Cosine</i>		0.567	0.289	0.397	0.563	0.307	0.371	0.048	0.193	0.222	0.171	79	0.057			
MSP- <i>Cosine</i> ^{SDR}		0.765	0.275	0.362	0.417	0.320	0.493	0.107	0.188	0.197	0.179	262	0.092			
MSP-ODIN		0.727	0.271	0.376	0.397	0.357	0.450	0.115	0.181	0.159	0.211	144	0.079			

Table 2: Comparison between state-of-the-art OWOD methods and the best FMap-based approaches discovered in RQ1, RQ2 and RQ3. Cells corresponding to the best values for each metric in each dataset are shaded in gray. In all metrics, higher values are better except for A-OSE and WI, for which lower values are better. The hyperparameter values of the FMap-based approaches are summarized in Table 3.

Method	Confidence Threshold	Cluster Method	Fusion Strategy
<i>Cosine</i>	0.100	HDBSCAN	-
<i>Cosine</i> ^{SDR}	0.010	KMeans ¹⁰	-
<i>Cosine</i> ^{SDR}	0.100	ONE	-
L_1^{EUL}	0.050	ONE	-
MSP	0.050	-	-
MSP- <i>Cosine</i>	0.050	HDBSCAN	OR
MSP- <i>Cosine</i> ^{SDR}	0.010	HDBSCAN	AND
MSP-ODIN	0.010	-	SCORE

Table 3: Hyperparameter values of the approaches included in Table 2.

6. Conclusions and Future Research Lines

This work has gravitated on the detection of unknown objects in single-stage object detector models, a problem that closely relates to the open-world object detection paradigm. Specifically, we have proposed a new unknown object detection method (FMap), which characterizes the feature maps extracted by object detection models to decide whether the object predictions issued by such models correspond to known (ID) or unknown (OoD) objects. In addition, we have designed two ways of improving the performance of the vanilla FMap method. The first reduces the dimensionality of extracted fea-

tures by capitalizing on existing SDR methods. The second, named EUL, aims to overcome the reduced capabilities of pretrained object detector to localize unknown objects by exploiting the information present in the feature maps computed by the model.

Subsequently, experiments have been run over the UOD benchmark [25] in response to four research questions, always bearing in mind a two-fold purpose: to detect unknown objects while maintaining a good detection on known classes. Different configurations of FMap in terms of distance metric, clustering method, the addition of SDR/EUL, and inference confidence threshold have been evaluated in terms of the trade-off between the aforementioned goals.

The main conclusions drawn from the experiments can be summarized as follows:

- Our experiments for RQ1 confirm that each version of the algorithm presented has its own unique advantages and disadvantages. The SDR method, for instance, excels in detecting unknown objects (high U-F1 values) and in providing robustness (measured by A-OSE), while preserving a satisfactory performance for known objects (measured by mAP). Conversely, integrating the EUL algorithm with FMap significantly enhances the detection of unknown objects, although this often results in a notable decrease in precision across many instances. The vanilla version obtained an acceptable balance between both objectives – known and unknown detection – without the additional complexity associated with the other two.
- Regarding RQ2, we have compared the best configurations of FMap against several post-hoc methods. The results showed that post-hoc methods generally lead to better known object detection capabilities for the same unknown object detection performance.
- To address RQ3, we have explored different fusion strategies between the considered OoD detection methods. For the fusion, we have developed three different possible strategies to elucidate the final outcome when participating methods disagree. Experiments evince that the ensemble of two post-hoc or logits-based techniques barely improve the results obtained by each of the methods independently. In contrast, when the fusion is between the proposed FMap and a post-hoc technique, a remarkable performance boost is achieved, outperforming the methods within the ensemble when applied separately. This demonstrates that logits- and feature-based

technique produce diverse yet complementary decisions, leading to a more robust detection of unknown objects.

- Finally, RQ4 has been answered by comparing some of the best configurations found in the previous experiments against state-of-the-art methods for unknown object detection and OWOD. Results have shown that FMap-based methods for single-stage object detectors consistently dominates the benchmark over known classes. Regarding the detection of unknowns, they have yielded superior recall statistics (ORE [5]) and F1 (UnSniffer [25]) scores, whereas one of FMap configurations have obtained the best precision. Furthermore, FMap-based methods have attained lower A-OSE and WI values, suggesting a reduced likelihood of misclassifying unknown objects as known. This robustness stems from our strategy of avoiding retraining, dramatically reducing the rate of object misclassifications.

To conclude, in this work we demonstrate how single-stage object detectors are inherently robust and how they can be easily endowed with decent unknown object detection capabilities compared to the SOTA. Moreover, we have designed an OoD or unknown object detection method for single-stage object detectors that obtains acceptable results and is very suitable for the fusion with the existing post-hoc methods.

In conclusion, this work has highlighted the inherent robustness of single-stage object detectors and their potential to be effectively enhanced with strong unknown object detection capabilities, standing competitively against state-of-the-art methods. Additionally, we have introduced a novel approach for unknown object detection, tailored for single-stage detectors, which achieves solid results when compared to existing post-hoc OoD methods. Our findings establish a new direction for further research and practical applications in open-world scenarios demanding safe and trustworthy AI deployments.

Future research lines. In future research, we aim to expand and refine the FMap method introduced in this manuscript. Its current implementation uses a straightforward algorithm to leverage the model’s extracted features. We envision enhancing this algorithm by exploring techniques to integrate features across different strides into a unified representation. Additionally, we plan to implement other SDR algorithms to further improve performance. Another promising avenue lies in the exploration of neural activations, particularly the activations derived from feature extraction components like feature

maps. These feature maps have shown considerable potential in OoD detection, whether used independently or combined with logits-based methods. We foresee manifold opportunities in this area (e.g. adversarial refinement of activations using latent interpolation), all recognizing their value for improving model robustness without requiring model retraining.

Acknowledgments

A. Martinez Seras receives funding support from the Basque Government through its BIKAINTEK PhD support program. J. Del Ser acknowledges funding support from the same institution through the Consolidated Research Group MATHMODE (IT1456-22) and the ELKARTEK program (BEREZ-IA, grant no. KK-2023/00012).

Appendix A. Results on Unknown Object Detection Benchmark

This appendix contains a table with the numerical results of all FMap configurations tested in our experiments.

Group	Method	Confidence threshold	Distance metric	Clustering method	Fusion strategy	mAP	U-AP	U-F1	U-PRE	U-REC	mAP	U-AP	U-F1	U-PRE	U-REC	A-OSE	WI
RQ1	FMap	0.050	L_1	ONE	-	0.662	0.152	0.209	0.578	0.127	0.435	0.022	0.111	0.216	0.075	368	0.141
RQ1	FMap	0.010	L_1	ONE	-	0.637	0.157	0.272	0.440	0.197	0.417	0.039	0.146	0.174	0.125	483	0.145
RQ1	FMap	0.005	L_1	ONE	-	0.620	0.200	0.203	0.381	0.238	0.407	0.039	0.152	0.152	0.151	536	0.142
RQ1	FMap	0.050	L_2	ONE	-	0.658	0.158	0.237	0.492	0.148	0.423	0.023	0.119	0.225	0.081	349	0.139
RQ1	FMap	0.010	L_2	ONE	-	0.640	0.204	0.287	0.451	0.211	0.410	0.040	0.148	0.177	0.127	470	0.141
RQ1	FMap	0.005	L_2	ONE	-	0.631	0.209	0.301	0.386	0.246	0.404	0.039	0.152	0.154	0.151	532	0.136
RQ1	FMap	0.010	L_2	Kmeans ¹⁰	-	0.629	0.225	0.331	0.412	0.277	0.341	0.042	0.173	0.162	0.186	284	0.118
RQ1	FMap	0.050	$Cosine$	ONE	-	0.658	0.158	0.237	0.392	0.148	0.423	0.023	0.119	0.225	0.081	349	0.139
RQ1	FMap	0.010	$Cosine$	ONE	-	0.640	0.204	0.287	0.451	0.211	0.410	0.040	0.148	0.177	0.127	470	0.141
RQ1	FMap	0.005	$Cosine$	ONE	-	0.631	0.209	0.301	0.386	0.246	0.404	0.039	0.152	0.154	0.151	532	0.136
RQ1	FMap	0.010	$Cosine$	Kmeans ¹⁰	-	0.629	0.225	0.331	0.412	0.276	0.341	0.042	0.173	0.162	0.185	285	0.118
RQ1	FMap	0.050	$L_{1/2}^{SOR}$	HDBSCAN	-	0.620	0.160	0.243	0.655	0.149	0.420	0.025	0.132	0.272	0.087	239	0.120
RQ1	FMap	0.010	$L_{1/2}^{SOR}$	HDBSCAN	-	0.637	0.219	0.327	0.431	0.264	0.385	0.045	0.169	0.173	0.165	349	0.125
RQ1	FMap	0.050	$L_{1/2}^{SOR}$	HDBSCAN	-	0.636	0.165	0.231	0.732	0.137	0.417	0.021	0.100	0.232	0.064	298	0.135
RQ1	FMap	0.005	$L_{1/2}^{SOR}$	ONE	-	0.635	0.167	0.271	0.617	0.171	0.409	0.021	0.117	0.218	0.080	350	0.144
RQ1	FMap	0.010	$L_{1/2}^{SOR}$	ONE	-	0.612	0.221	0.323	0.424	0.261	0.407	0.038	0.152	0.160	0.145	550	0.134
RQ1	FMap	0.050	$L_{1/2}^{SOR}$	ONE	-	0.597	0.164	0.248	0.713	0.150	0.411	0.022	0.114	0.240	0.075	270	0.127
RQ1	FMap	0.010	$L_{1/2}^{SOR}$	ONE	-	0.581	0.223	0.333	0.480	0.255	0.395	0.040	0.161	0.185	0.143	424	0.133
RQ1	FMap	0.005	$L_{1/2}^{SOR}$	ONE	-	0.573	0.224	0.334	0.408	0.238	0.391	0.041	0.163	0.161	0.164	484	0.129
RQ1	FMap	0.010	$Cosine^{SOR}$	ONE	-	0.527	0.258	0.351	0.668	0.238	0.380	0.051	0.164	0.275	0.116	155	0.087
RQ1	FMap	0.050	$Cosine^{SOR}$	ONE	-	0.477	0.292	0.389	0.453	0.352	0.327	0.062	0.191	0.181	203	206	0.086
RQ1	FMap	0.010	$Cosine^{SOR}$	Kmeans ¹⁰	-	0.520	0.241	0.362	0.663	0.249	0.370	0.049	0.168	0.266	0.123	142	0.082
RQ1	FMap	0.050	$Cosine^{SOR}$	Kmeans ¹⁰	-	0.507	0.241	0.384	0.381	0.287	0.357	0.047	0.180	0.235	0.115	166	0.085
RQ1	FMap	0.010	$Cosine^{SOR}$	Kmeans ¹⁰	-	0.471	0.296	0.392	0.427	0.363	0.323	0.061	0.190	0.174	0.209	185	0.082
RQ1	FMap	0.050	$Cosine^{SOR}$	HDBSCAN	-	0.533	0.241	0.351	0.667	0.238	0.376	0.051	0.165	0.276	0.118	155	0.089
RQ1	FMap	0.010	$Cosine^{SOR}$	HDBSCAN	-	0.519	0.241	0.377	0.587	0.278	0.366	0.049	0.178	0.244	0.140	180	0.092
RQ1	FMap	0.050	$Cosine^{SOR}$	HDBSCAN	-	0.478	0.295	0.388	0.432	0.352	0.329	0.062	0.190	0.180	0.202	211	0.091
RQ1	FMap	0.010	$L_{1/2}^{FULL}$	ONE	-	0.602	0.161	0.254	0.239	0.270	0.435	0.031	0.119	0.099	0.150	368	0.141
RQ1	FMap	0.050	$L_{1/2}^{FULL}$	ONE	-	0.637	0.203	0.277	0.241	0.327	0.417	0.031	0.132	0.101	0.190	483	0.145
RQ1	FMap	0.005	$L_{1/2}^{FULL}$	ONE	-	0.629	0.206	0.282	0.233	0.358	0.407	0.040	0.134	0.098	0.212	536	0.142
RQ1	FMap	0.010	$L_{1/2}^{FULL}$	Kmeans ¹⁰	-	0.529	0.225	0.287	0.234	0.371	0.341	0.051	0.144	0.103	0.240	284	0.118
RQ1	FMap	0.050	$Cosine^{FULL}$	Kmeans ¹⁰	-	0.529	0.225	0.287	0.234	0.371	0.341	0.049	0.144	0.103	0.239	285	0.118
RQ1	FMap	0.010	$Cosine^{FULL}$	HDBSCAN	-	0.577	0.217	0.282	0.234	0.356	0.385	0.046	0.139	0.102	0.218	349	0.125
RQ2	MSP	0.050	-	-	-	0.719	0.237	0.390	0.565	0.298	0.446	0.083	0.186	0.237	0.153	123	0.073
RQ2	MSP	0.001	-	-	-	0.724	0.319	0.289	0.206	0.483	0.448	0.107	0.136	0.086	0.329	135	0.078
RQ3	MSP-FMap	0.050	$Cosine$	HDBSCAN	OR	0.467	0.289	0.397	0.463	0.307	0.371	0.048	0.193	0.222	0.171	70	0.057
RQ3	MSP-FMap	0.005	$Cosine$	HDBSCAN	AND	0.775	0.280	0.314	0.354	0.282	0.501	0.113	0.160	0.152	0.169	445	0.120
RQ3	MSP-FMap	0.005	$L_{1/2}^{SOR}$	ONE	AND	0.788	0.302	0.287	0.116	0.220	0.513	0.112	0.149	0.178	0.138	501	0.126
RQ3	MSP-FMap	0.001	$L_{1/2}^{SOR}$	ONE	AND	0.780	0.307	0.282	0.276	0.288	0.516	0.112	0.150	0.125	0.188	822	0.113
RQ3	MSP-FMap	0.010	$Cosine^{SOR}$	HDBSCAN	AND	0.765	0.275	0.362	0.417	0.320	0.493	0.107	0.158	0.197	0.179	262	0.092
RQ3	MSP-FMap	0.050	-	-	OR	0.702	0.289	0.399	0.367	0.308	0.431	0.077	0.188	0.228	0.100	107	0.069
RQ3	MSP-ODIN	0.010	-	-	OR	0.702	0.289	0.399	0.367	0.381	0.437	0.094	0.184	0.157	0.223	107	0.069
RQ3	MSP-ODIN	0.050	-	-	AND	0.734	0.270	0.375	0.397	0.355	0.456	0.109	0.179	0.158	0.206	159	0.085
RQ3	MSP-ODIN	0.010	-	-	SCORE	0.727	0.271	0.376	0.397	0.357	0.450	0.115	0.181	0.159	0.211	144	0.079

Table A.4: Results from best configurations of the methods from RQ1, RQ2 and RQ3

References

- [1] Y. Bengio *et al.*, “Managing extreme ai risks amid rapid progress,” *Science*, vol. 384, no. 6698, pp. 842–845, 2024.
- [2] High-level Expert Group on Artificial Intelligence, “Ethics guidelines for trustworthy AI,” *European Commission*, available at: <https://digital-strategy.ec.europa.eu/en/library/ethics-guidelines-trustworthy-ai>, 2019.
- [3] N. Díaz-Rodríguez, J. Del Ser, M. Coeckelbergh, M. Lopez de Prado, E. Herrera-Viedma, and F. Herrera, “Connecting the dots in trustworthy Artificial Intelligence: From AI principles, ethics, and key requirements to responsible AI systems and regulation,” *Information Fusion*, vol. 99, p. 101896, 2023, publisher: Elsevier.
- [4] E. Tabassi, “Artificial intelligence risk management framework (AI RMF 1.0),” 2023.
- [5] K. Joseph, S. Khan, F. S. Khan, and V. N. Balasubramanian, “Towards open world object detection,” in *IEEE/CVF Conference on Computer Vision and Pattern Recognition*, 2021, pp. 5830–5840.
- [6] D. K. Singh *et al.*, “Order: Open world object detection on road scenes,” in *Neural Information Processing Systems (NeurIPS) Workshops*, vol. 1, 2021, p. 3, issue: 2.
- [7] X. Zhao, Y. Ma, D. Wang, Y. Shen, Y. Qiao, and X. Liu, “Revisiting open world object detection,” *IEEE Transactions on Circuits and Systems for Video Technology*, vol. 34, no. 5, pp. 3496–3509, 2024.
- [8] Y. Wang, Z. Yue, X.-S. Hua, and H. Zhang, “Random boxes are open-world object detectors,” in *IEEE/CVF International Conference on Computer Vision*, 2023, pp. 6233–6243.
- [9] A. Martinez-Seras, J. Del Ser, J. L. Lobo, P. Garcia-Bringas, and N. Kasabov, “A novel out-of-distribution detection approach for spiking neural networks: design, fusion, performance evaluation and explainability,” *Information Fusion*, vol. 100, p. 101943, 2023.

- [10] Y. Sun, C. Guo, and Y. Li, “React: Out-of-distribution detection with rectified activations,” *Advances in Neural Information Processing Systems (NeurIPS)*, vol. 34, pp. 144–157, 2021.
- [11] R. Huang, A. Geng, and Y. Li, “On the importance of gradients for detecting distributional shifts in the wild,” *Advances in Neural Information Processing Systems*, vol. 34, pp. 677–689, 2021.
- [12] D. Hendrycks and K. Gimpel, “A baseline for detecting misclassified and out-of-distribution examples in neural networks,” *International Conference on Learning Representations (ICLR)*, 2017.
- [13] S. Liang, Y. Li, and R. Srikant, “Enhancing the reliability of out-of-distribution image detection in neural networks,” *arXiv preprint arXiv:1706.02690*, 2017.
- [14] W. Liu, X. Wang, J. Owens, and Y. Li, “Energy-based out-of-distribution detection,” *Advances in Neural Information Processing Systems (NeurIPS)*, vol. 33, pp. 21 464–21 475, 2020.
- [15] X. Du, Z. Wang, M. Cai, and Y. Li, “Vos: Learning what you don’t know by virtual outlier synthesis,” *arXiv preprint arXiv:2202.01197*, 2022.
- [16] X. Du, X. Wang, G. Gozum, and Y. Li, “Unknown-aware object detection: Learning what you don’t know from videos in the wild,” in *IEEE/CVF Conference on Computer Vision and Pattern Recognition*, 2022, pp. 13 678–13 688.
- [17] S. Wilson, T. Fischer, F. Dayoub, D. Miller, and N. Sünderhauf, “SAFE: Sensitivity-aware features for out-of-distribution object detection,” in *IEEE/CVF International Conference on Computer Vision and Pattern Recognition*, 2023, pp. 23 565–23 576.
- [18] A. Zolfi, G. Amit, A. Baras, S. Koda, I. Morikawa, Y. Elovici, and A. Shabtai, “YolOOD: Utilizing object detection concepts for multi-label out-of-distribution detection,” in *IEEE/CVF Conference on Computer Vision and Pattern Recognition*, 2024, pp. 5788–5797.
- [19] A. Dhamija, M. Gunther, J. Ventura, and T. Boulton, “The overlooked elephant of object detection: Open set,” in *IEEE/CVF Winter Conference on Applications of Computer Vision*, 2020, pp. 1021–1030.

- [20] M. Everingham, L. Van Gool, C. K. Williams, J. Winn, and A. Zisserman, “The pascal visual object classes (VOC) challenge,” *International Journal of Computer Vision*, vol. 88, pp. 303–338, 2010.
- [21] T.-Y. Lin, M. Maire, S. Belongie, J. Hays, P. Perona, D. Ramanan, P. Dollár, and C. L. Zitnick, “Microsoft COCO: Common objects in context,” in *Computer Vision—ECCV 2014: 13th European Conference, Zurich, Switzerland, September 6–12, 2014, Proceedings, Part V 13*. Springer, 2014, pp. 740–755.
- [22] A. Gupta, S. Narayan, K. Joseph, S. Khan, F. S. Khan, and M. Shah, “OW-DETR: Open-world detection transformer,” in *IEEE/CVF Conference on Computer Vision and Pattern Recognition*, 2022, pp. 9235–9244.
- [23] J. R. Uijlings, K. E. Van De Sande, T. Gevers, and A. W. Smeulders, “Selective search for object recognition,” *International Journal of Computer Vision*, vol. 104, pp. 154–171, 2013.
- [24] Z. Wu, Y. Lu, X. Chen, Z. Wu, L. Kang, and J. Yu, “UC-OWOD: Unknown-classified open world object detection,” in *European Conference on Computer Vision*, 2022, pp. 193–210.
- [25] W. Liang, F. Xue, Y. Liu, G. Zhong, and A. Ming, “Unknown Sniffer for Object Detection: Don’t Turn a Blind Eye to Unknown Objects,” in *IEEE/CVF Conference on Computer Vision and Pattern Recognition*, 2023, pp. 3230–3239.
- [26] T.-Y. Lin, P. Dollár, R. Girshick, K. He, B. Hariharan, and S. Belongie, “Feature pyramid networks for object detection,” in *IEEE/CVF Conference on Computer Vision and Pattern Recognition*, 2017, pp. 2117–2125.
- [27] K. He, G. Gkioxari, P. Dollár, and R. Girshick, “Mask R-CNN,” in *IEEE International Conference on Computer Vision*, 2017, pp. 2961–2969.
- [28] N. Otsu, “A threshold selection method from gray-level histograms,” *IEEE Transactions on Systems, Man, and Cybernetics*, vol. SMC-9, no. 1, pp. 62–66, 1979.

- [29] D. Miller, L. Nicholson, F. Dayoub, and N. Sünderhauf, “Dropout sampling for robust object detection in open-set conditions,” in *IEEE International Conference on Robotics and Automation (ICRA)*, 2018, pp. 3243–3249.
- [30] G. Jocher, A. Chaurasia, and J. Qiu, “Ultralytics YOLO,” Jan. 2023. [Online]. Available: <https://github.com/ultralytics/ultralytics>
- [31] B. Szubert, J. E. Cole, C. Monaco, and I. Drozdov, “Structure-preserving visualisation of high dimensional single-cell datasets,” *Scientific Reports*, vol. 9, no. 1, p. 8914, 2019.